NUMERICAL STUDY OF NATURAL MELT CONVECTION IN CYLINDRICAL CAVITY WITH HOT WALLS AND COLD BOTTOM SINK

by

Abdennacer AHMANACHE [a]* and Noureddine ZERAIBI [b]

[a] Centre for Development of Advanced Technologies, Baba Hassen, Algiers, Algeria
[b] University M´Hamed Bougara of Boumerdes, Boumerdes, Algeria

Original scientific paper
DOI: 10.2298/TSCI110327166A

Numerical study of natural convection heat transfer and fluid flow in cylindrical cavity with hot walls and cold sink is conducted. Calculations are performed in terms of the cavity aspect ratio, the heat exchanger length, and the thermo physical properties expressed via the Prandtl and the Rayleigh numbers. Results are presented in the form of isotherms, streamlines, average Nusselt number, and average bulk temperature for a range of Rayleigh number up to 10^6. It is observed that Rayleigh number and heat exchanger length influences fluid flow and heat transfer, whereas the cavity aspect ratio has no significant effects.

Key words: *numerical heat transfer, natural convection, fluid flow*

Introduction

Natural convective heat transfer in an enclosure has been studied extensively because of the wide applications of such process in numerous engineering applications, such as solar energy systems, cooling of electronic circuits, air conditioning, crystal growth, and many others. Therefore it is very important for applied research as comprehensively reviewed by Ostrach [1] and Bejan [2]. The literature survey on this class of problem is fairly exhaustive. Considerable efforts have been exerted to deal with different boundary conditions occurring in practice. Ganzarolli and Milanez [3] studied natural convection in an enclosure heated from below and symmetrically cooled from the sides, Lemembre and Petit [4] investigated a cylinder insulated at the bottom, laterally heated at a uniform heat flux density and cooled at the same flux at the top surface, Aydin *et al.* [5] investigated the influence of aspect ratio for air-filled rectangular enclosures heated from one side and cooled from the top, Corcione [6] studied natural convection in a air-filled rectangular enclosure heated from below and cooled from above for a variety of thermal boundary conditions at the side walls, recently Basak *et al.* [7] investigated steady laminar natural convection flow in a square cavity with uniformly and non-uniformly heated bottom wall, and adiabatic top wall maintaining constant temperature of cold vertical walls. Other authors consider natural convection induced by localized heating sources. Sezai and Mohamad [8] studied numerically natural convection from a discrete flush-mounted rectangular heat source on the bottom of a horizontal enclosure, the enclosure is cooled from above and insulated from the bottom, effect of vertical boundary conditions on the rate of heat transfer from the heat source is studied, Aydin and Yang [9] and Sharif and Mohammad [10] numerically investigated the natural convection of air in a vertical square cavity with localized isothermal and

* Corresponding author; e-mail: aahmanache @cdta.dz

isoflux heating from below and symmetrical cooling from sidewalls. The top wall and the non-heated parts of the bottom wall were considered adiabatic. Deng *et al.* [11] studied numerical natural convection in a rectangular enclosure with discrete heat sources on walls. Sun and Emery [12] studied conjugate natural convection heat transfer in a 2-D air-filled enclosure containing discrete internal heat sources and an internal baffle, while Ha and Jung [13] investigated the problem of conjugate heat transfer of natural convection and conduction in a vertical differentially heated cubic enclosure within which a centered, cubic, heat-conducting body generates heat. Liaqat and Baytas [14] analyzed numerically a square enclosure having thick conducting walls filled with a Bousinessq fluid with a Pr of 7.0 containing uniform volumetric sources.

All the studies mentioned above are dealing with heated walls or localized single/multiple sources or inner volumetric sources. The present study is based on cylindrical cavity filled with melted material heated from walls and with localized bottom cold sink. Such configuration is encountered in heat exchanger method (HEM) [15] a crystal growth furnaces. Melt convection plays a central role in bulk crystal growth because it influences the heat and mass transfer which in turn influences and controls the important growth features, like shape and position of the solid-liquid interface, chemical composition of the growth crystal and density and distribution of dislocations and strain in the crystal. Melt convection in crystal growth can be driven by three mechanisms, viz.: buoyancy-driven convection, forced convection and capillary (Marangoni) convection. Several excellent reviews which have discussed the importance of fluid motion and convective heat transfer in crystal growth systems have been published by Pimputkar and Ostrach [16], Hurle [17], Brown [18], Derby [19], Muller and Ostrogorsky [20]. Although much effort has been made to study the convection phenomena in melt crystal growth systems, like Czochralski, Bridgman, and floating zone techniques, in order to improve the crystal quality and to understand the crystal growth process, see [20] for extensive bibliography. The HEM which is, comparatively, a new promising simple directional solidification technique, has received little attention [21-23]. At he present time this technique is used to grow large multicrystalline silicon ingot for photovoltaic purpose [24, 25].The HEM is a process which controls both the heat input and the heat extraction independently in a crystal growth furnace. The HEM is a process which controls both the heat input and the heat extraction independently in a crystal growth furnace. The HEM crystal growth process includes the following steps: heating the material to above the melting point, then solidifying the melted material by extracting heat from the central portion of the bottom of the crucible. The amount of heat removed by the heat exchanger is controlled by the flow rate of helium gas.

The aim of this paper is to investigate numerically the effects of the cavity aspect ratio, the heat exchanger length and the thermo physical properties of the material expressed via the Prandtl and Rayleigh numbers on natural melt convection occurring in HEM furnace. The schematic diagram of physical system along with the computational domain employed in the present study is shown in fig. 1. The computation domain is limited to the crucible-melt system. It consists of a cylindrical enclosure of dimension $H \times W$ whose walls are kept at a constant hot temperature T_H, and the heat exchanger with length L, in the bottom of the cavity, is kept at constant cold temperature T_C. The cavity aspect ratio is defined as $A = H/W$. With this geometry and boundary conditions, the present study reports the computations for cavities at aspect ratios 0.5, 1, 1.5, and 2. The ratio of the heat exchanger length to the cavity width L/W, which is subsequently designated as ε was varied from 0.1 to 1. Ra was varied from 10^3 to 10^6. Effects of these parameters on heat transfer and fluid flow are analyzed for an oxide material BGO ($Bi_4Ge_3O_{12}$) with Pr = 20 [26], and results are presented in terms of isotherms, stream functions, average Nusselt number at the heat exchanger and bulk average temperature of the cavity.

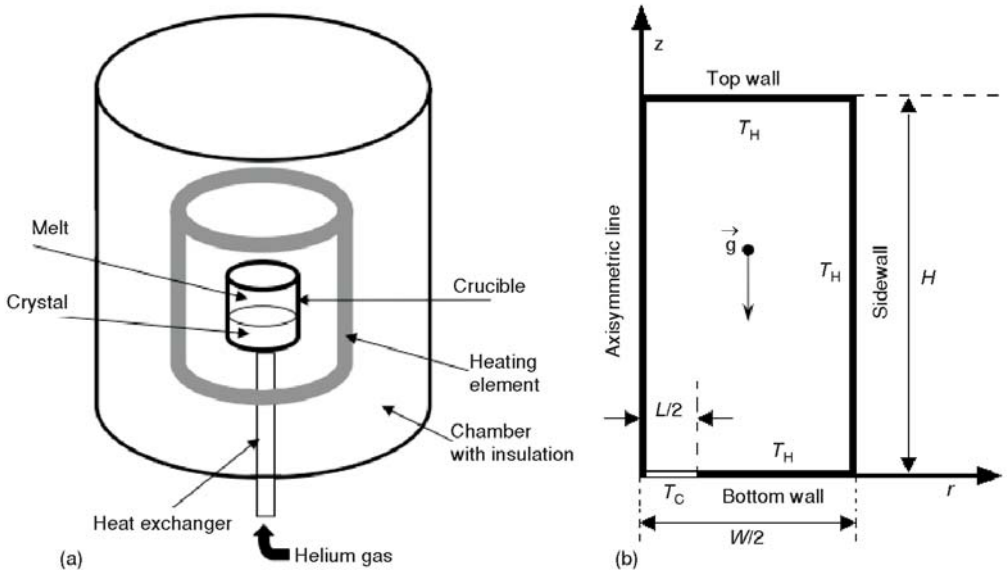

Figure 1. (a) Schematic diagram of the physical system, (b) Computational domain employed in the present study

Mathematical formulation

The computational domain, reduced to the crucible, is shown in fig. 1(b). It is assumed that temperature and flow fields are axisymmetric, this allows for a 2-D model, therefore only half of the geometry is considered. The fluid is assumed to be laminar, steady-state, Newtonian, and incompressible. All thermophysical properties of the fluid are assumed to be constant except for the density in the buoyancy term of the momentum equation in the vertical direction, which is treated by using the Boussinesq approximation. With these assumptions the governing equations in dimensionless cylindrical co-ordinates form are then given as follows:

– continuity equation

$$\frac{1}{r}\frac{\partial(ru)}{\partial r}+\frac{\partial v}{\partial z}=0 \tag{1}$$

– momentum equation

$$u\frac{\partial u}{\partial r}+v\frac{\partial u}{\partial z}=-\frac{\partial p}{\partial r}+\mathrm{Pr}\left[\frac{\partial}{\partial r}\left(\frac{1}{r}\frac{\partial}{\partial r}(ru)\right)+\frac{\partial^2 u}{\partial z^2}\right] \tag{2}$$

$$u\frac{\partial v}{\partial r}+v\frac{\partial v}{\partial z}=-\frac{\partial p}{\partial r}+\mathrm{Pr}\left[\frac{1}{r}\frac{\partial}{\partial r}\left(r\frac{\partial v}{\partial r}\right)+\frac{\partial^2 v}{\partial z^2}\right]+\mathrm{Ra}\,\mathrm{Pr}\,\theta \tag{3}$$

– energy equation

$$u\frac{\partial \theta}{\partial r}+v\frac{\partial \theta}{\partial z}=\frac{1}{r}\frac{\partial}{\partial r}\left(r\frac{\partial \theta}{\partial r}\right)+\frac{\partial^2 \theta}{\partial z^2} \tag{4}$$

where u and v are velocity components in the r- and z-directions, respectively, p is the pressure, and θ – the temperature.

Non-dimensional quantities are obtained as:

$$r = \frac{R}{W}, \quad z = \frac{Z}{W}, \quad u = \frac{U}{U_o}, \quad v = \frac{V}{U_o}, \quad p = \frac{P}{\rho U_0^2}, \quad \theta = \frac{T - T_C}{T_H - T_C} \tag{5}$$

where $U_o = \alpha/W$ is a characteristic velocity, ρ and α are the fluid density and the thermal diffusivity, respectively, and T_C and T_H, the temperatures of cold heat exchanger and hot walls. Pr = ν/α, and Ra = $g\beta(T_H - T_C)W^3/\nu\alpha$ are the dimensionless parameters governing the flow, where ν – the kinematic viscosity, β – the thermal expansion coefficient of the fluid, and g – the gravitational acceleration in z direction.

The boundary conditions for the present problem are specified as:

– at top wall, sidewall, and bottom wall:

$$u = v = 0, \quad \theta = 1 \tag{6}$$

– at heat exchanger

$$u = v = 0, \quad \theta = 0 \tag{7}$$

– at axisymmetric line

$$\left.\frac{\partial\theta}{\partial r}\right|_{r=0} = \left.\frac{\partial u}{\partial r}\right|_{r=0} = \left.\frac{\partial v}{\partial r}\right|_{r=0} = 0 \tag{8}$$

The local Nusselt number at the cold heat exchanger is computed as:

$$\mathrm{Nu}(r) = -\frac{\partial\theta}{\partial r} \tag{9}$$

The dimensionless stream function is defined such that:

$$u = \frac{1}{r}\frac{\partial\psi}{\partial z}, \quad v = -\frac{1}{r}\frac{\partial\psi}{\partial r} \tag{10}$$

Numerical method

The governing eqs. (1)-(4), along with boundary conditions, are solved using the finite volume technique. The pressure-velocity coupling is achieved using the Simple method. First order upwind scheme is used to discretize the momentum and energy equations. Under relaxation factors for energy and momentum equations are varied to achieve convergence for high Ra numbers. The convergence criterion is that the maximal residual of all the governing equations is less than 10^{-6}.

A systematic grid independence study was conducted to select proper grid resolution for all cases. It was found that grid independence is achieved with dimensionless space step equal to $6.25 \cdot 10^{-3}$, beyond which the change in average Nusselt number, bulk average temperature and maximum stream function is less than 0.5%.

The normalized length ε of the heat exchanger was varied from 0.1 to 1 by 0.1 step. For each value of ε, the Ra was varied from 10^3 to 10^6. Four aspect ratios have been used A = 0.5, 1.0, 1.5 and 2.0. Thus a total of 160 simulations were computed.

The computations presented in this article could not be validated against experiment due to the lack of experimental data for the specific configurations investigated here. However, benchmark solutions of De Vahl Davis [27] and numerical results of Markatos [28] for natural convection in differentially heated square cavity for Ra ranging from 10^3 to 10^6 were reproduced and excellent agreement was found, as we can see in tab. 1.

Table 1. Validations of present study benchmark solutions [27] and numerical results [28] for buoyancy-driven flow in a square, differentially heated cavity. ($u_{max.}$ and $v_{max.}$ are calculated on the vertical mid-plane (respectively horizontal mid-plane) of the square cavity.)

Ra	Reference	$\overline{Nu}$	$Nu_{max.}$	$u_{max.}$	$v_{max.}$
10^3	[28]	1.118	1.505	3.649	3.697
	[29]	1.108	1.496	3.544	3.593
	Present study	1.095	1.509	3.615	3.661
10^4	[27]	2.243	3.528	16.178	19.617
	[28]	2.201	3.482	16.18	19.617
	Present study	2.203	3.561	16.132	19.394
10^5	[27]	4.519	7.717	34.73	68.59
	[28]	4.430	7.626	35.73	69.08
	Present study	4.470	7.875	35.466	68.044
10^6	[27]	8.800	17.925	64.63	219.36
	[28]	8.754	17.872	68.81	221.80
	Present study	8.851	18.665	67.329	217.739

Results and discussion

Effects of aspect ratio of the cavity, Rayleigh number and dimensionless heat ex-changer size on fluid flow, thermal fields, average Nusselt number and bulk average temperature in the whole cavity are illustrated and discussed. Because of space limitation, it is not possible to include the results for all Ra for various ε and aspect ratios, only some representative streamlines and isotherms are shown in fig. 2 and figs. 4-6. Figure 3 resumes effect of aspect ratio of the cavity. The summary of the results of simulations for all cases are presented in figs. 7-8 in the form of maximal stream function, average Nusselt number and average bulk fluid temperature in the cavity in terms of Rayleigh number and dimensionless length of heat exchanger.

Effect of aspect ratio

The effects of aspect ratio are illustrated in figs. 3 and 4. Streamlines and isotherms are shown in fig. 3 for Ra = 10^6 and for ε = 0.2 and 0.7, as a representative cases. Resume of all simulation are depicted in fig. 3. We can see that flow field

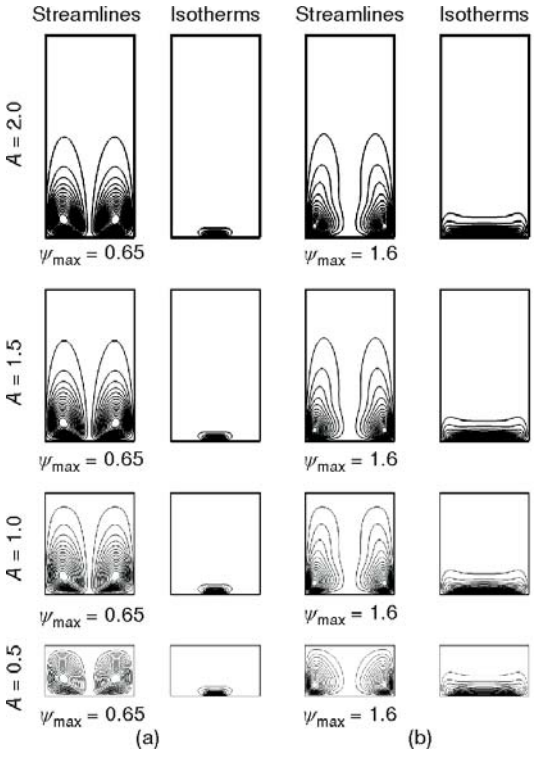

Figure 2. Streamlines and isotherms for different aspect ratio with Ra = 10^6; (a) ε = 0.2, (b) ε = 0.7

and thermal fields, in this kind of cavity, are not sensitive to the aspect ratio variation whatever are Ra and ε. Therefore we will restrict our discussion in the following upcoming results on the case $A = 1$.

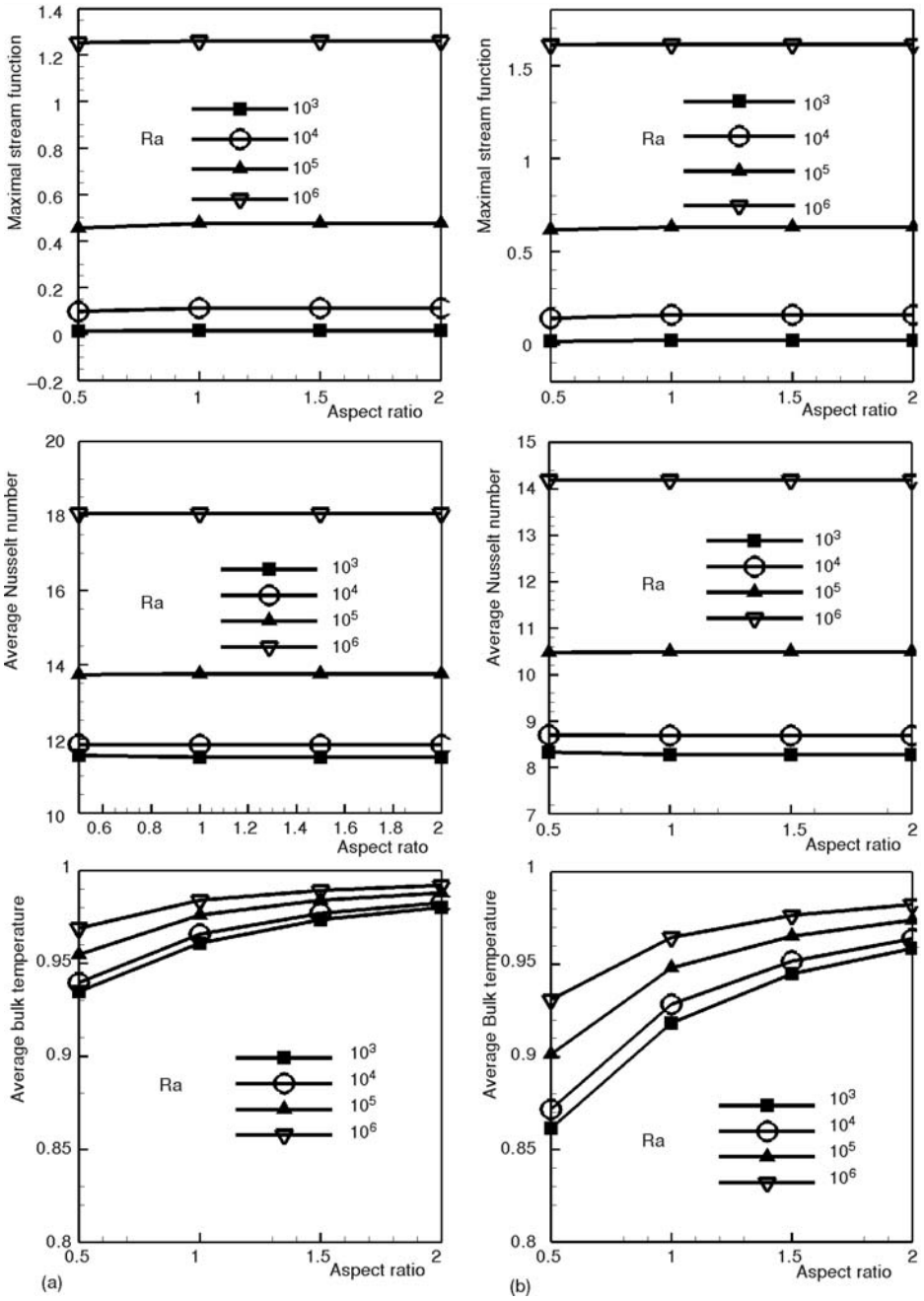

Figure 3. Variation of maximal stream function, average Nusselt number and average bulk temperature with aspect ratio for various Ra; (a) $\varepsilon = 0.4$, (b) $\varepsilon = 0.6$

Effects of varying the Rayleigh number on the flow field and on the heat transfer

We consider first the effect of varying the Rayleigh number. The resulting flow and temperature distribution are depicted in fig. 4-6 for some representative cases. The flow is downward at the centerline, reaches the cold heat exchanger at the bottom of the cavity and then rises along the hot walls creating two symmetrical counter-rotating rolls in the cavity. The isotherms are symmetrical about the centerline and are concentrated, with increasing Ra, towards the heat exchanger keeping the whole cavity at uniform temperature. For lower Ra ($\leq 10^4$), conduction is the principal mode of heat transfer as suggested by the parabolic form of the isotherms and the low value of maximal stream function. When increasing Ra (10^5 and 10^6) the value of the maximal stream function increases significantly, the core of the counter-rotating rolls moves down and shifts to the corner of the cavity and the isotherms are flattened suggesting that convection mode becomes dominant. Figure 7 summarizes the effect of Ra for all simulations. We can see that, for a given ε, maximal stream function increases considerably for $Ra > 10^4$ confirming the predominance of convection mode. The average Nusselt number $\overline{Nu}$ also increases with Ra for a given value of ε. When Ra is less then 10^4 $\overline{Nu}$ grows only slightly with increasing Ra. After Ra is more than 10^4 $\overline{Nu}$ is found to increase more rapidly suggesting that the natural convection aids more and more in the heat transfer process in addition to the conduction. The bulk average temperature increases with Ra as shown in fig. 7. In fact increasing Ra, for a given material, results from increasing heating: $Ra \propto T_H - T_C$ and therefore increasing the heating of the cavity for a given ε.

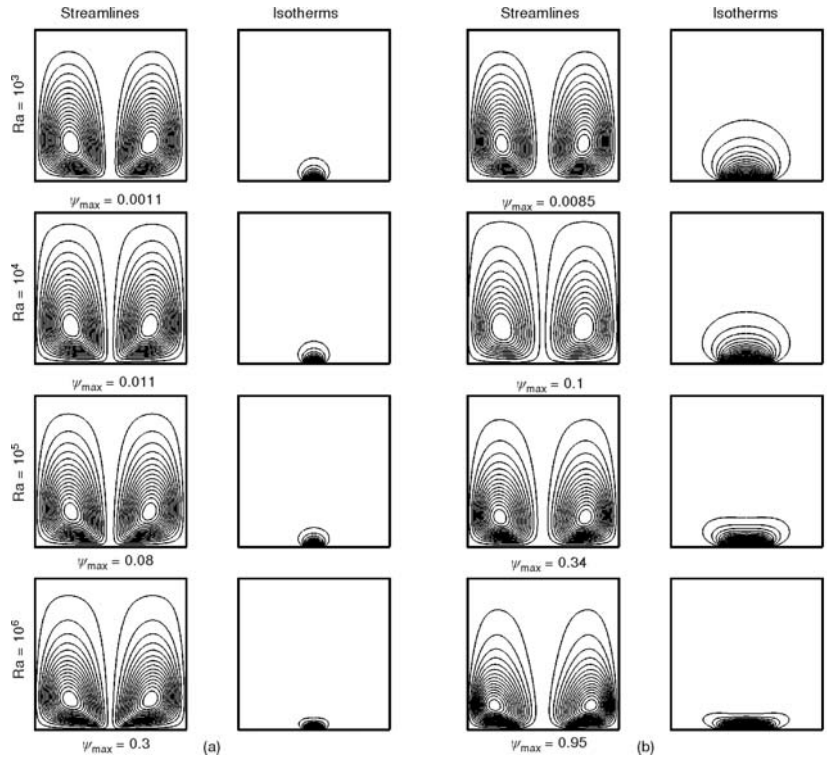

Figure 4. Streamlines and isotherms in the cavity with $A = 1$; (a) $\varepsilon = 0.1$, (b) $\varepsilon = 0.3$

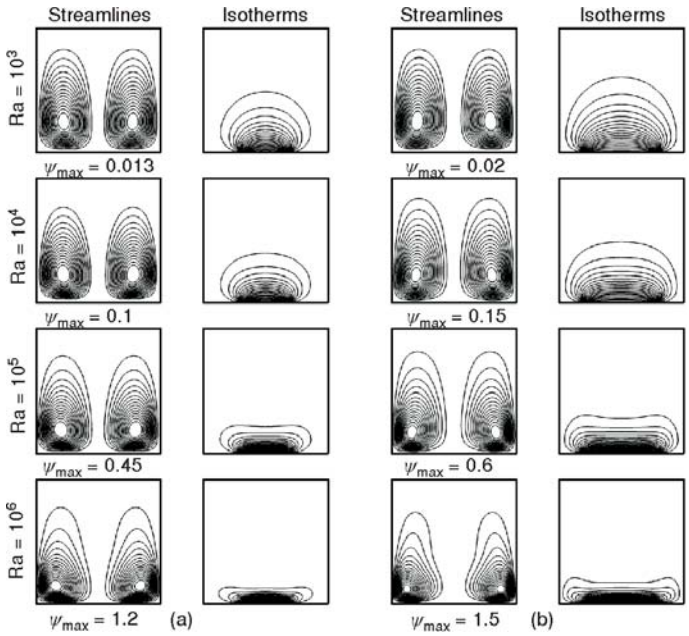

Figure 5. Streamlines and isotherms in the cavity with $A = 1$ (a) $\varepsilon = 0.4$, (b) $\varepsilon = 0.6$

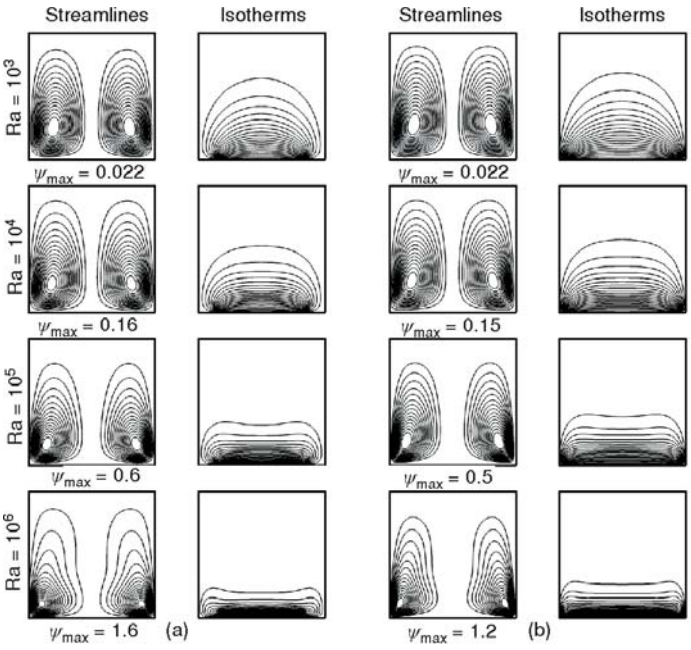

Figure 6. Streamlines and isotherms in the cavity with $A = 1$ (a) $\varepsilon = 0.7$, (b) $\varepsilon = 0.9$

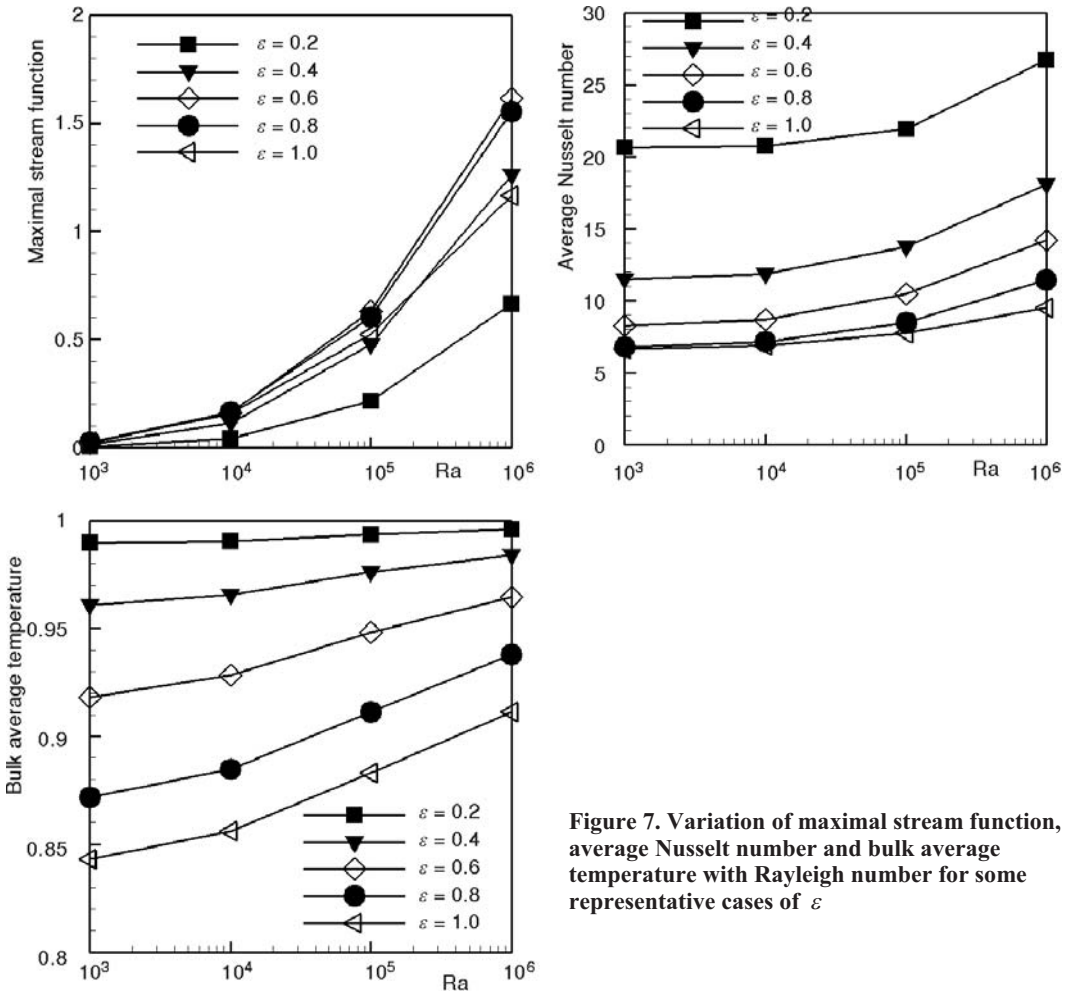

Figure 7. Variation of maximal stream function, average Nusselt number and bulk average temperature with Rayleigh number for some representative cases of ε

Effects of varying the dimensionless length of heat exchanger on the flow field and on the heat transfer

Now we discuss the effect of the dimensionless length of the heat exchanger ε on the fluid flow and on the heat transfer. Results are summarized in fig. 8 where variations of maximal stream function, average Nusselt number and average bulk temperature $\overline{\theta}$ are reported in terms of ε. The length of the heat exchanger has an interesting effect on the intensity of the convection for a given Ra. Indeed the maximal stream function increases with ε, reaches a maximum for ε = 0.7 then decreases. The fluid particles reaching the bottom of the cavity, along the centerline, are accelerated by the cold heat exchanger and then slowed down by the hot walls. More long is the path traveling of the particles in the heat exchanger more they are accelerated. Up to ε = 0.7 the effect of the heat exchanger is more important and particles are accelerated, beyond ε = 0.7 the effect of the hot walls are predominant and particles are slowed down.

The average Nusselt number decreases with ε for a given Ra. In fact, as we can see in figs. 5-7, isotherms are more flattened and concentrated near the cold wall for small ε, increasing the temperature gradient near the heat exchanger and thus increasing the heat exchanger co-

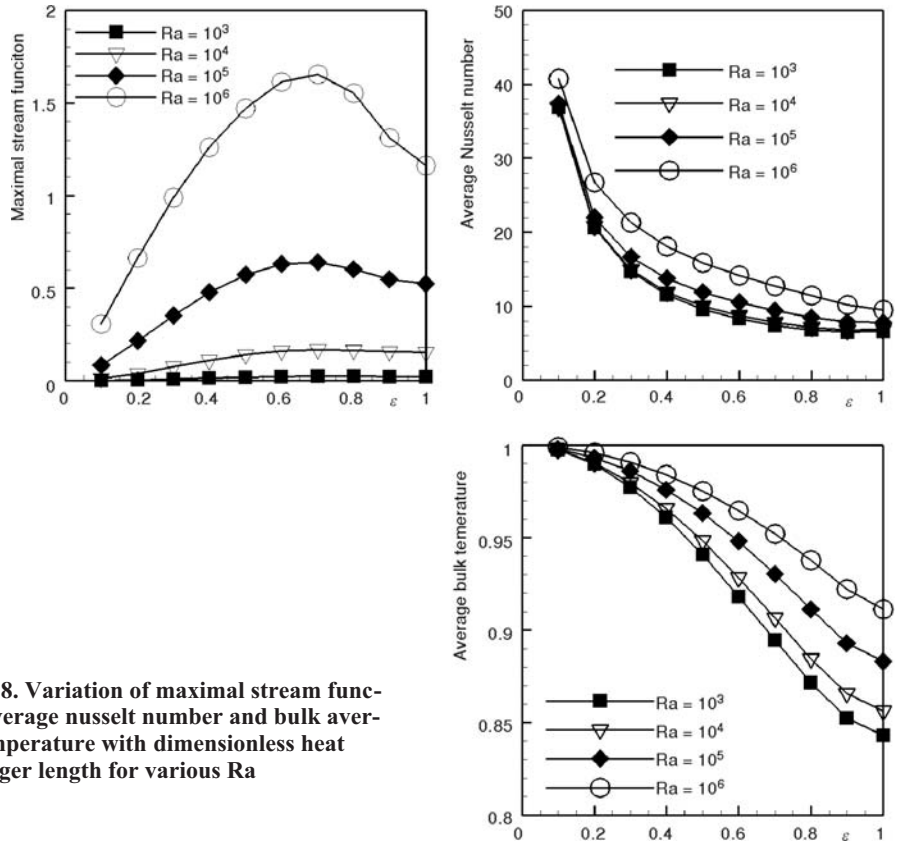

Figure 8. Variation of maximal stream function, average nusselt number and bulk average temperature with dimensionless heat exchanger length for various Ra

efficient h, which in turn increases the Nusselt and the average Nusselt numbers. The average bulk temperature of the cavity decreases with ε, for a given Ra, because more surface is brought into play and more heat is evacuated through the heat exchanger.

Conclusions

In the present paper a numerical study of natural convection in a cylindrical cavity filled with melted material heated from walls and cooled from a localized bottom sink has been conducted. Such configuration is encountered in HEM: a crystal growth furnace. The main parameters of interest are Ra = 10^3 to 10^6, Prandtl number, dimensionless heat sink length (ε = 0.1 to 1), and cavity aspect ratio (A = 0.5, 1.0, 1.5, and 2.0). A total of 160 computations have been computed. Stream functions, isotherms, average Nusselt number, and bulk average temperature have been used to study the effect of parameters on fluid flow and heat transfer.

The following conclusions may be drawn from the present study:

- Aspect ratio, up to A = 2, has no significant effect on fluid flow and heat transfer in such cavity.
- The governing parameters affecting fluid flow and heat transfer are Rayleigh number and heat exchanger length. For Ra < 10^4, the flow and heat transfer is dominated by conduction, for Ra > 10^5 convection plays the major role.

- The dimensionless heat exchanger length has an interesting effect on the intensity of the convection. The maximal stream function increases with ε, reaches a maximum and then decreases due to the competitive role of the heating walls and the cooling heat exchanger.
- Average Nusselt number decreases with the dimensionless length of the heat exchanger.

Nomenclature

A – aspect ratio of the cavity, (= H/W)
g – gravitational acceleration, [ms^{-2}]
H – height of the cavity, [m]
h – heat transfer coefficient, [Wm^{-2}K^{-1}]
L – length of the heat exchanger, [m]
$\overline{\mathrm{Nu}}$ – average Nusselt number (= $(1/\varepsilon)\int_0^{\varepsilon}\mathrm{Nu}(r)\mathrm{d}r$
P – pressure, [Pa]
p – dimensionless pressure, (= $P/(\rho U_0^2)$)
Pr – Prandtl number, (= ν/α)
R – radial co-ordinates, [m]
Ra – Rayleigh number [= $(\beta g/\nu\alpha)(T_H - T_C)W^3$]
r – dimensionless radial co-ordinate, (= R/W)
T – temperature, [K]
T_C – cold temperature, [K]
T_H – hot temperature, [K]
U – radial velocity, [ms^{-1}]
U_0 – characteristic velocity, (= α/W)
u – dimensionless radial velocity, (= U/U_0)
V – longitudinal velocity, [ms^{-1}]
Vol – volume of the cavity, [m^3]
v – dimensionless longitudinal velocity (= V/U_0)
W – width of the cavity, [m]
z – dimensionless longitudinal co-ordinate (= Z/W)
Z – longitudinal co-ordinate, [m]

Greek symbols

α – thermal diffusivity, [m^{2}s^{-1}]
β – coefficient of volume expansion, [K^{-1}]
ε – dimensionless length of the heat exchanger, (= L/W)
θ – dimensionless temperature: $(T - T_C)/(T_H - T_C)$
$\bar{\theta}$ – bulk temperature: [=$1/Vol\int_{Vol}\theta\mathrm{d}(Vol)$]
ν – kinematics viscosity, [m^{2}s^{-1}]
ρ – fluid density, [kgm^{-3}]
ψ – dimensionless stream function

Subscripts

H – hot
C – cold

References

[1] Ostrach, S., Natural Convection in Enclosures, *J. Heat Transfer, 110* (1988), 43, pp. 1175-1190
[2] Bejan, A., *Convection Heat Transfer*, John Wiley & Sons, New York, USA, 1982
[3] Ganzarolli, M.M., Milanez, L. F., Natural Convection in Rectangular Enclosures Heated from Below and Symmetrically Cooled from the Sides, *Int. J. Heat Mass Transfer, 38* (1995), 6, pp.1063-1073
[4] Lemembre, A., Petit, J. P., Laminar Natural Convection in a Laterally Heated and Upper Cooled Vertical Cylindrical Enclosure, *Int. J. Heat Mass Transfer, 41* (1998), 16, pp. 2437-2454
[5] Aydin, O., *et al*., Natural Convection in Rectangular Enclosures Heated from One Side and Cooled from the Ceiling, *Int. J. Heat Mass Transfer, 42* (1999), 13, pp. 2345-2355
[6] Corcione, M., Effects of the Thermal Boundary Conditions at the Sidewalls Upon Natural Convection in Rectangular Enclosures Heated from Below and Cooled from Above, *Int. J. Thermal Sciences, 42* (2003), 2, pp. 199-208
[7] Basak, T., *et al*., Effects of Thermal Boundary Conditions on Natural Convection Flows within a Square Cavity, *Int. J. Heat Mass Transfer, 49* (2006), 23-24, pp. 4525-4535
[8] Sezai, I., Mohamad, A. A., Natural Convection from a Discrete Heat Source on the Bottom of a Horizontal Enclosure, *Int. J. Heat Mass Transfer, 43* (2000), 13, pp. 2257-2266
[9] Aydin, O., Yang, J., Natural Convection in Enclosures with Localized Heating from Below and Symmetrical Cooling from Sides, *Int. J. Numer. Methods Heat Fluid Flow, 10* (2000), 5, pp. 518-529
[10] Sharif, M. A. R., Mohammad, T. R., Natural Convection in Cavities with Constant Flux Heating at the Bottom Wall and Isothermal Cooling from Sidewalls, *Int. J. Thermal Sciences, 44* (2005), 9, pp. 865-878
[11] Deng, Q. H., *et al*., A Combined Temperature Scale for Analyzing Natural Convection in Rectangular Enclosures with Discrete Wall Heat Sources, *Int. J. Heat Mass Transfer, 45* (2002), 16, pp. 3437-3446

[12] Sun, Y. S., Emery, A. F., Effects of Wall Conduction, Internal Heat Sources and an Internal Baffle on Natural Convection Heat Transfer in a Rectangular Enclosure, *Int. J. Heat Mass Transfer, 40* (1997), 4, pp. 915-929
[13] Ha, M. Y., Jung, M. A., Numerical Study on Three-Dimensional Conjugate Heat Transfer of Natural Convection and Conduction in a Differentially Heated Cubic Enclosure with a Heat-Generating Cubic Conducting Body, *Int. J. Heat Mass Transfer, 43* (2000), 23, pp. 4229-4248
[14] Liaqat, A., Baytas, A. C., Conjugate Natural Convection in a Square Enclosure Containing Volumetric Sources, *Int. J. Heat Mass Transfer, 44* (2001), 17, pp. 3273-3280
[15] Schmid, F., Crystal Growing, US patent No 3898051, 1975
[16] Pimputkar, S. M., Ostrach, S., Convective Effects in Crystals Grown from Melt, *J. Crystal Growth, 55* (1981), 3, pp. 614-646
[17] Hurle, D. T. J., Convective Transport in Melt Growth Systems, *J. Crystal Growth, 65* (1983), 1-3, pp. 124-132
[18] Brown, R. A., Theory of Transport Processes in Single Crystal Growth from the Melt, *AIChe Journal, 34* (1988), 6, pp. 881-911
[19] Derby, J. J., An Overview of Convection During the Growth of Single Crystals from the Melt, Anonymous *Proceedings*, 8th International Summer School on Crystal Growth, ISSCG-8, Japan, 1992
[20] Muller, G., Ostrogorsky, A. G., Convection in Melt Growth, in: *Handbook of Crystal Growth* (Eds. D. T. J. Hurle), Elsevier Science Pub. Co, vol. 2, 1994
[21] Wang, J. H., *et al.*, Modelling of Crystal Growth Process in Heat Exchanger Method, *J. Crystal Growth, 174* (1997), 1-4, pp. 13-18
[22] Lu, C. W., Chen, J. C., Numerical Computation of Sapphire Crystal Growth Using Heat Exchanger Method, *J. Crystal Growth, 225* (2001), 2-4, pp. 274-281
[23] Chen, J.-C., Lu, C.-W. , Influence of the Crucible Geometry on the Shape of the Melt-Crystal Interface during Growth of Sapphire Crystal Using a Heat Exchanger Method, *J. Crystal Growth, 266* (2004), 1-3, pp. 239-245
[24] Kim, J. M., Kim, Y. K., Growth and Characterization of 240 kg Multicrystalline Silicon Ingot Grown by Directional Solidification, *Solar Energy Materials & Solar Cells, 81* (2004), 2, pp. 217-224
[25] Khattak, C. P., Schmid, F., Growth of the World's Largest Sapphire Crystals, *J. Crystal Growth, 225* (2001), 2-4, pp. 572-579
[26] Evstratov, I. Y., *et al*., Global Analysis of Heat Transfer in Growing BGO Crystals (Bi4Ge3O12) by Low-Gradient Czochralski Method, *J. Crystal Growth, 235* (2002), 1-4, pp. 371-376
[27] De Vahl Davis, G., Natural Convection of Air in a Square Cavity: A benchmark Solution, *Int. J. Numer. Meth. Fluids, 3* (1983), 3, pp. 249-264
[28] Markatos, N., Pericleous, K. A., Laminar and Turbulent Natural Convection in an Enclosed Cavity, *Int. J. Heat Mass Transfer, 27* (1984), 5, pp. 755-772

Paper submited: March 27, 2011
Paper revised: September 25, 2012
Paper accepted: September 25, 2012